Biomechanical behavior of the dental implant macrodesign in mandibular implant-supported overdentures

G. S. OKKAN[1], S. KÜÇÜKKURT[3], H. TERZİOĞLU[4], N. MOLLAOĞLU[2]

[1]DDS PhD - Private Practice, Ankara, Turkey
[2]DDS PhD - Professor, Gazi University, Department of Oral and Maxillofacial Surgery, Ankara, Turkey
[3]DDS PhD - Associate Professor, Istanbul Aydın University, Department of Oral and Maxillofacial Surgery, Istanbul, Turkey
[4]DDS PhD - Professor, Ankara University, Department of Prosthetic Dentistry, Ankara, Turkey

TO CITE THIS ARTICLE
Okkan GS, Küçükkurt S, Terzi'oğlu H, Mollaoğlu N. Biomechanical behavior of the dental implant macrodesign in mandibular implant-supported overdentures. J Osseointegr 2021;13(4):234-241.

DOI 10.23805 /JO.2021.13.04.9

KEYWORDS Dental Implants, Implant-Supported Denture, Finite Element Analysis.

ABSTRACT

Aim The present *in vitro* study aimed to evaluate the effect of different dental implant macrodesigns on the stress occurred on the implants and bone for two-implant-supported overdentures (IOD) in the rehabilitation of edentulous mandibles.
Methods Six different implant brands and macro design were used in this study. Two groups, Group V (V-thread shape) and Group R (reverse buttress thread shape), were formed based on implant thread shape. Vertical and oblique loads were applied to the implants in order to evaluate tension, compression, and Von Mises stresses by implementing the three-dimensional finite element analysis.
Results According to the stresses after the applied forces, the macrodesign of dental implants affects stress distribution in different directions. Group R exerted more stresses on the cortical bone, while Group V produced more stresses on the implants. Tissue level implants caused high stresses on bones and low stress on itself. As proposed, microthread neck design decreased the stresses on the cortical bone.
Conclusion In the light of these biomechanical findings, considering the anterior region of the mandible often consists of dense cortical bone, it may be advantageous to prefer implants with a V-thread design and a microthread neck surface, which creates less stress in the cortical bone.

INTRODUCTION

Implant-supported overdentures (IODs) are better than the conventional removable prostheses, especially with regard to retention and stability.1 Patients using IODs present with comparatively fewer oral health problems, higher satisfaction concerning their chewing ability, and better retention, as compared to the patients using conventional removable prostheses (1, 2). These advantages often make IODs a preferred treatment method.
The load transmitted from the dental implant to the surrounding bone depends on the type of force applied, the bone-implant interface, the length and diameter of the implant, the macro- and microgeometry of the implant, and the density of the surrounding bone. The stresses introduced by these loads may affect the osseointegration and functional life of the dental implants (3-8).
The effect of implant macrogeometry on the success of dental implants have been described in many studies (5, 9). The functions of implant threads include providing retention and primary stabilization, increasing the implant surface area, and better distribution of stress in the peri-implant bone (8). Surface features like threads, pores, grooves, and steps on the implants facilitate mechanical locking between the implant and bone tissue (4,7,8). It is, therefore, necessary to understand how the thread shape and geometry of dental implants affect the burden on bone and, therefore, the stresses, in each case (10).
The literature reports only a few studies that have examined the effect of implant macrodesign on IOD prostheses for stress distribution. This study hypothesized that load transmitted to the IODs may be affected by implant macrodesign, which might contribute to treatment planning and implant selection. This was examined by placing six implants with different macrodesign on virtual mandibles in pairs and, the stresses occurred by the models were analyzed using finite element analysis (FEA), upon force application.

MATERIALS AND METHODS

Models

For the present in vitro study, six virtual mandible models were created. The models were classified into two groups based on the thread properties of the implants. The implants with V-thread (triangular) were placed in Group V and, implants with reverse buttress threads were placed in Group R. Besides, all implants of Group R had a wider thread pitch than those of Group V. While model V-As had micro-threaded neck surface, model R-Bi had a sloped neck, and model R-Sw and R-St were tissue level implants and had machined-surface neck designs with different lengths (R-Sw: 2.5 mm, R-St: 1.8 mm). The two groups were also divided into subgroups, and each model was named utilizing the first two letters of the implant brand. The properties of the implants used in the models are presented in Table 1.

Modeling

Computed tomography images of a completely edentulous mandible were obtained from a patient. The images were converted into DICOM (Digital Imaging and Communications in Medicine) format by the inclusion of 1-mm diameter sections. These sections were recorded using computer software (Rhinoceros 5.0; Robert McNeel and Associates) that produced a model of the edentulous alveolar crest, prosthetic base, implants, and ball attachments. The mandible was modeled as a D2 type of bone, i.e., trabecular bone covered with a 1-mm outer cortical layer. The bone thickness of 1.5 mm was formed surrounding the implants.
Six different types of implants and ball attachments were scanned with a three-dimensional scanner (Activity 880; Smart Optics, Sensortechnik GmbH, Bochum, Germany), and datasets were created in stereolithographic (.stl) format. Rhinoceros 5.0 software was used to create the models. Implants were placed symmetrically, in pairs, on the virtual mandibles in the area of the canines (Fig. 1). The present study attempted to standardize the diameter and length of the implants by using the option closest to the 4.2 mm diameter and 10 mm length, in the framework of the existing designs of implant manufacturers. In each model, the superstructure comprised standard ball attachments with a 2 mm gingival height.
In order to obtain the most realistic results, the number of nodes is as high as possible. In mathematical models, 4-node tetrahedral solid (solid tetrahedral solid pyramid) elements are preferred and these elements are distributed homogeneously in each model. In this study, during the preparation of mathematical models including the mandible, the implants and prosthetic base, the number of elements between 663,742 and 1,586,878 and the number of nodes between 120,026 and 276,092 were used.

Boundary and loading conditions

The models were constrained at the nodes on the cross-sectional areas behind the retromolar pads in all degrees of freedom. Modeled structures were simulated as tightly bonded. It was assumed that load transfers were performed according to the internal properties of cortical and trabecular bone. The connection between the implants and the supporting tissues, the relationship between the ball attachments and implants, and the ball attachments and prosthesis were designed to transfer loads directly. Additionally, the overdentures and attachments were assumed

MODEL		IMPLANT	NECK	THREAD SHAPE	THREAD
NAME	IMPLANT BRAND	TYPE	REGION		PITCH
			GROUP V		
V-As	Astratech Osseospeed Tx	Bone level	Microthreaded (0.2 mm)	V-thread	0.6 mm
V-St	Straumann				
	Bone level	Bone level	No	V-thread	0.7 mm
V-Xi	Dentsply Xive	Bone level	No	V-thread	0.8 mm
			GROUP R		
R-Bi	Bicon Integra	Bone level	Sloping	Reverse buttress	1 mm
R-Sw	SwissPlus	Tissue level	Machined surface (2.5 mm)	Reverse buttress	1.2 mm
R-St	Straumann				
Tissue Level	Tissue level	Machined surface (1.8 mm)	Reverse buttress	1.2 mm	

TABLE 1 The brand, type and thread properties of the implants used in the models. Group V: V-threaded implants used in this study (V-As, V-St and V-Xi). Group R: Reverse buttress threaded implants used in this study (R-Bi, R-St and R-Sw).

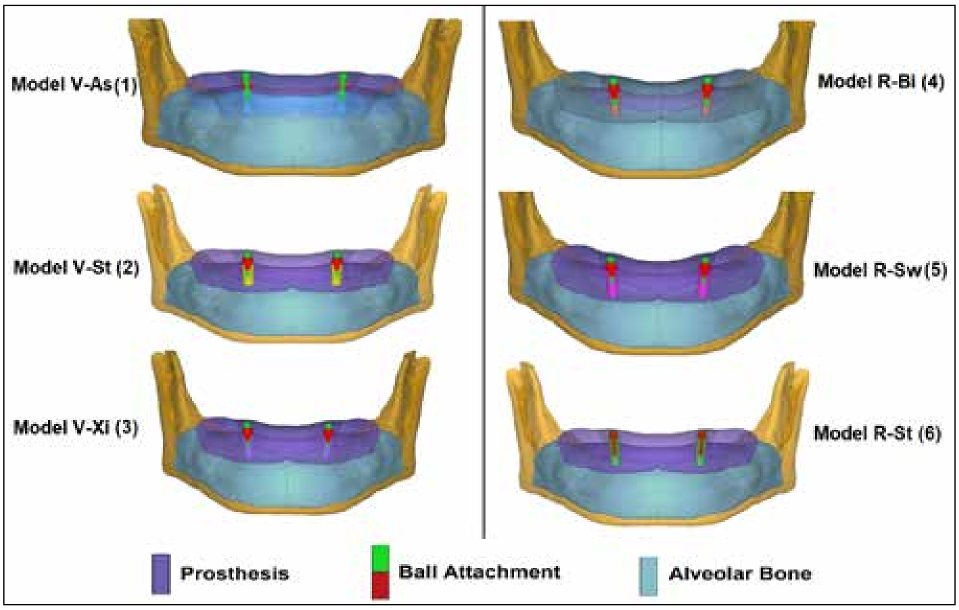

FIG 1 Models created for this study. Model V-As: Model with V-threaded Astratech Osseospeed Tx® implants. Model V-St: Model with V-threaded Straumann Bone Level® implants. Model V-Xi: Model with V-threaded Dentsply Xive® implants. Model R-Bi: Model with Reverse buttress threaded Bicon Integra® implants. Model R-St: Model with Reverse buttress threaded Straumann Tissue Level® implants. Model R-Sw: Model with Reverse buttress threaded SwissPlus® implants.

to be in perfect contact, and the friction coefficient was ignored. The implants were assumed to be 100% osseointegrated. All materials used in this study were defined as homogeneous, isotropic, and linear elastic. Material properties determined for acrylic resin, mucosa, cortical bone, trabecular bone, and implants are shown in Table 2 (11).

In FEA studies, it is necessary to apply forces in a proper direction and amount so that the stresses generated are closest to reality (10, 12, 13). As described in a similar study (11), for each model, two occlusal loads (100 N) were applied to the prosthetic base; vertically and obliquely at an angle of 30° from the center of the buccal cusp of the first molar of the overdenture unilaterally in buccolingual direction. The loads applied on the overdentures were assumed static, and vertical loads were directed on the central fossa of the right and the left first molar teeth, unilaterally and bilaterally

	Material	Young's modulus (MPa)	Poisson's ratio
Implants	Titanium (TiAl4V)	103400	0.35
Ball attachment	Titanium (TiAl4V)	103400	0.35
Prosthesis	Acrylic resin	3000	0.35
Cortical bone	-	13700	0.30
Trabecular bone	-	1370	0.30
Mucosa	-	1	0.37

TABLE 2 Material properties.

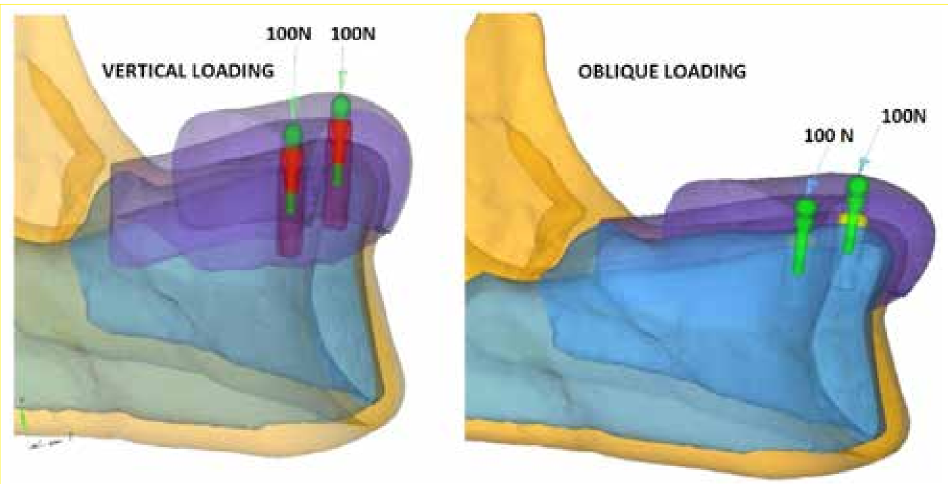

FIG. 2 Loading conditions.

(Fig. 2).

Analysis

In order to assess the effects of different framework materials and loading on stress distribution, von Mises stresses (σvM) were calculated for dental implants and maximum (σmax) (tensile) and minimum (σmin) (compression) principal stresses were calculated for peri-implant bone (14). To quantify the highest stress values the node with the maximum value in any model was selected for each structure. While obtaining this value, the smoothing function of the software was used. The stress value of a node is defined by the average stress occurring in a node adjacent to a given node by this function, in this way possible errors are minimized. Stress values were automatically calculated in megapascals (MPa) using the software's range, color and magnitude scales.

Algor FemPro (Algor Inc. Pittsburgh, USA) software was used for the analysis of the data. Since the data obtained from finite element analysis are mathematical calculations without variance, the results were not statistically analyzed; they were evaluated with scales instead. All stress values were represented using color and quantity scales. The results were evaluated in comparative terms (Fig. 4-8).

RESULTS

Vertical loadings

The evaluation of Pmax (Maximum principal stress, Tension stress) in the cortical bone revealed that more stress ensued in Group V than in Group R. Model V-As was the subgroup that encountered the maximum stress (16.3 MPa). Conversely, Pmin (Minumum principal stress, Compression stress) in the cortical bone was observed to be higher in Group R. Model R-Sw was the subgroup with the maximum Pmin value (–31.5 MPa) (Fig. 2, 6, 7).

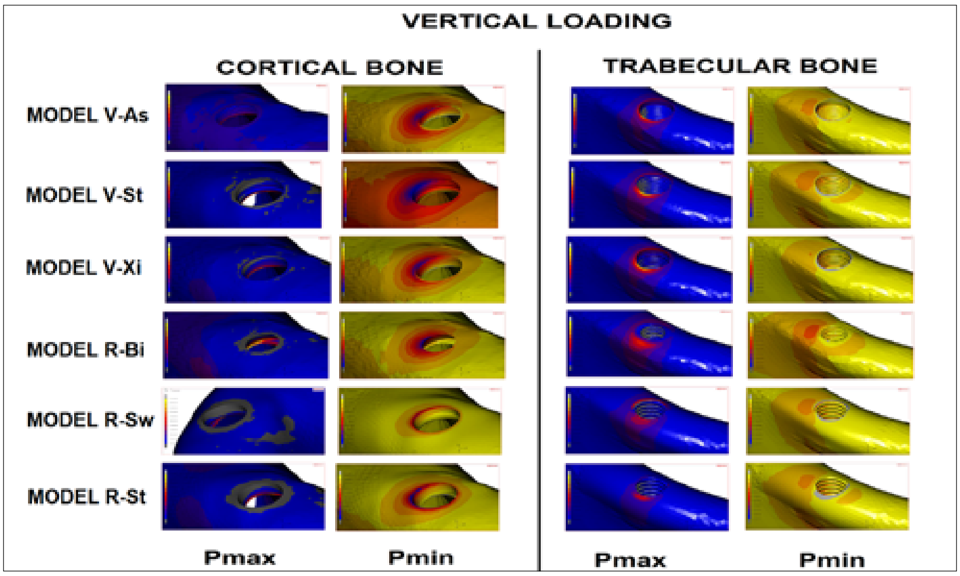

FIG. 3 Compression and tension stresses in cortical and trabecular bone against vertical loading.

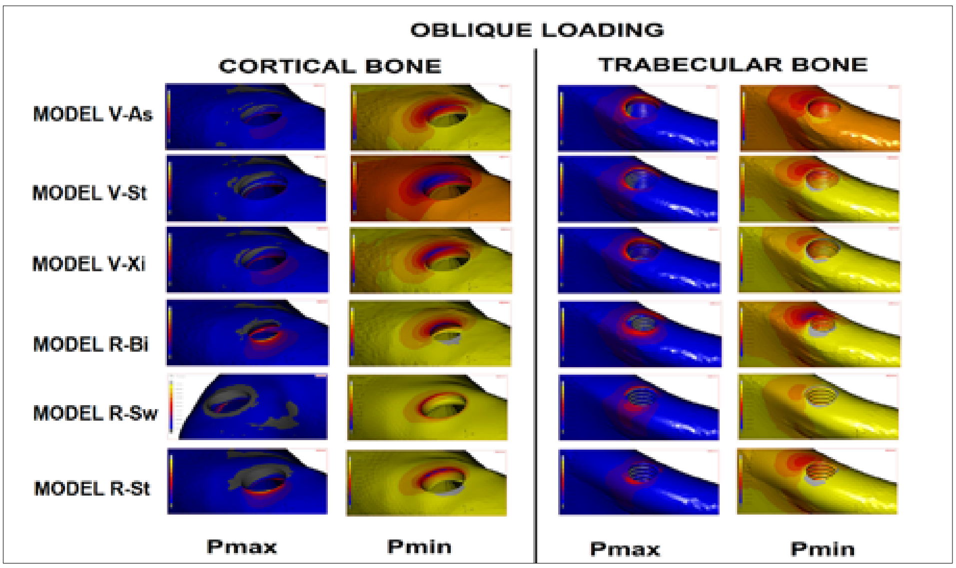

FIG. 4 Compression and tension stresses in cortical and trabecular bone against oblique loading.

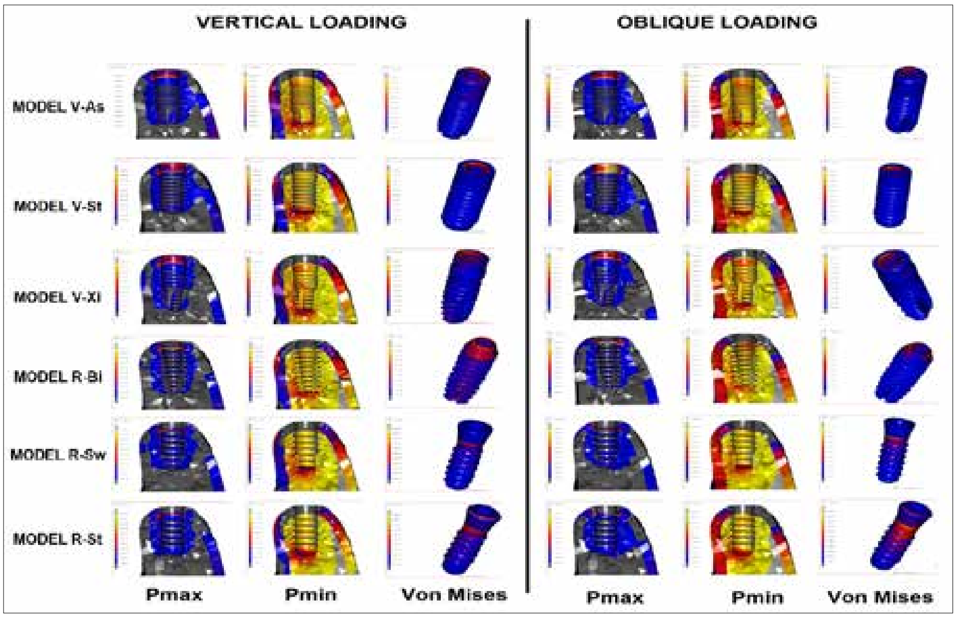

FIG. 5 Compression and tension stresses in peri-implant bone and von Mises stresses observed in implants against vertical and oblique loadings.

On the other hand, Pmax values in the trabecular bone were observed to be close to each other in all models except for model R-St (3.8 MPa). In terms of Pmin values in the trabecular bone, the stresses were also observed to be close to each other. Besides, the highest stress was measured in model V-Xi (–3.2 MPa), while the lowest stress was measured in model R-Bi (–2 MPa) (Fig. 2, 6, 7).

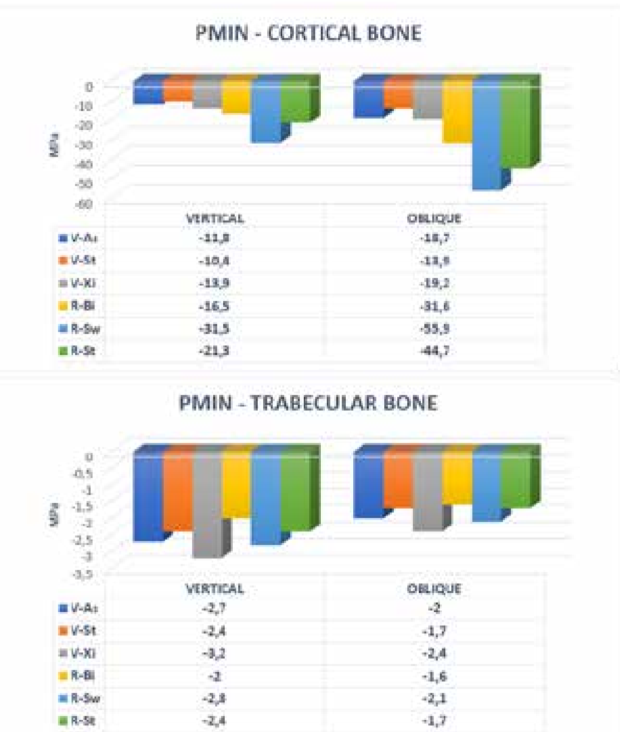

FIG. 7 Compression stresses (Pmin) in cortical and trabecular bone against vertical and oblique loading.

Oblique loadings

The analysis of Pmax values in the cortical bone showed that while stress distribution between the groups was relatively stable, the highest stresses were measured in model R-Sw (21.2 MPa), and the lowest stresses were measured in model V-Xi (11.7 MPa). Differently, for Pmin, it was observed that more stress developed in Group R. Maximum stress was reported in model R-Sw (–55.9 MPa) and model R-St (–44.7 MPa), while least stress was detected in model V-St (–13.9 MPa) (Fig. 3, 6, 7).

On comparing Pmax values in the trabecular bone, stresses were found to be balanced in Group V models and one of Group R model (R-Bi), while higher stresses were measured in the other two models of Group R (model R-Sw with 3.2 MPa and model R-St with 2.1 MPa). Besides, Pmin stresses in the models were found to be balanced. While the highest stress developed in model V-Xi (–2.4 MPa), the lowest stress ensued in model R-Bi (–1.6 MPa) (Fig. 3, 6, 7).

FIG. 8 Von Mises stresses (MPa) in implants and ball attacments against vertical and oblique loading.

Von Mises Stress

Contrary to the vertical forces, it was found that the stress intensities in Group V were higher. Especially in Model V-St, the stress was 139 MPa, which was nearly 2.5 times more than that in the nearest Model R-Sw (55.9 MPa). Similarly, against oblique forces, the stresses in Group V were higher, with Model R-St showing the highest value (329 MPa) which was two times higher than in Model V-As (159.7 MPa). In both conditions, Model R-St had the lowest stresses (Vertical: 31.6 MPa and Oblique: 50 MPa). In general, the oblique forces caused more stresses around the implants (Fig. 4, 8).

DISCUSSION

Implant thread properties have a pronounced effect on the bone-implant surface area, stress distributions, and implant stability (6, 15, 16). Abuhussein et al. (3) reported that the V-thread and square-thread implant types exerted lesser stress on the trabecular bone. Lima de Andrade et al. (8) reported that thread design is the main factor governing trabecular bone stress and that V-thread produces the lowest stress in trabecular bone. Mosavar et al. (13) reported that square threads showed the most favorable results compared to buttress, reverse buttress and V-thread designs according to the predicted values of von Mises equivalent stress, pressure, different shear stresses, and micromotion.

In the present study, reverse buttress implants produced higher Pmax stress in the trabecular bone, whereas V-thread implants produced higher Pmin stress. In the cortical bone, reverse buttress implants generated higher stresses under all conditions, except for Pmax stress-induced against the vertical cutting forces. In biomechanical terms, the Pmax forces had considerably higher values and, oblique forces reflecting grinding forces, which requires a longer duration, were more important than the vertical loadings, which simulated a shorter food cutting activity. Besides, in two implant-supported mandibular overdenture evaluated in our study, implants were placed in the anterior region of the mandible. Both Lekholm and Zarb's classification (17) and Misch's classification (18) indicate that the anterior mandibular region is usually D1 (>1250 Hounsfield units) and mainly consists of cortical bone. Therefore, the results of the present study imply that V-thread implants presented improved biomechanical behavior in terms of stress formations on the bone.

Kong Liang et al. (15) argued that increasing the thread pitch is a more compelling factor for controlling stress distribution in the trabecular bone. Researchers emphasize that the minimum stress ensues when the thread pitch is less than 0.7 mm for cortical bone and more than 0.8 mm in case of trabecular bone. Lan et al. (19) advocated a thread pitch exceeding 0.8 mm is more appropriate for a screwed implant. In the present study, V-thread implants were employed with an average of 0.7 mm thread pitch, while reverse buttress implants had an average of 1.1 mm thread pitch. In the cortical bone, implants with higher thread pitch induced higher stresses in all conditions except for Pmax stress on cortical bone against cutting forces. In trabecular bone, implants with higher thread pitch produced higher Pmax stress, while implants with lower thread pitch generated higher Pmin stress. These results support those obtained by Kong Liang et al. (15).

Lan et al. (19) reported that the main effects of stresses exerted on the implants depend on the thread pitch and the oblique forces; however, the thread shape does not affect stress distribution. Similar to Lan et al. (19), the present study also demonstrated that oblique forces produce higher stresses in the cortical bone. Against to the oblique forces, reverse buttress and higher thread pitch implants induced higher stress under almost all conditions, as long as Pmin stress in the trabecular bone was lower. On the other hand, the highest von Mises stress, against oblique forces, was observed in the V-Thread and lower thread pitch implants. Therefore, although the results of the present study support those of Lan et al. (19), the point of contention is that thread shape also affects stress distributions, as observed in this study.

Yalçın et al. (20) stated that the microthreads on the implant crest module might cause an increase in stress to cortical bone surrounding the neck region of implants. Despite that, Al-Thobity et al. (21) reported that lesser crestal bone was lost with dental implants that had a micro-threaded neck design in comparison to those with machined-surface or conventional rough-surface dental implants. Thus, the researchers stated that micro-threaded dental implants are a better choice than implants with other designs. Nickenig et al. (22) established that rough-surfaced micro-threaded design caused a significantly lesser loss of crestal bone under long-term functional loading in the mandible when compared to machined-neck implants. In the present study, Model V-As with micro-thread neck caused low stresses in the cortical bone under almost all conditions, especially against oblique forces. The high-stress formation was observed only in the Pmax stresses against vertical forces. In these conditions, micro-threaded neck design can be considered to contribute to the reduction of resorption by reducing stresses occurring in the cervical collar in the cortical bone.

Markose et al. (23) stated that the implants with a sloping shoulder is much favorable for bone growth, stress distribution, and preservation of the remaining bone. In another study, the same researchers also reported that short implants with sloping shoulder designs have superior survival rates as compared to regular implants (24). Considering the stresses that occurred on the cortical bone in the present study, the findings of model R-Bi with the sloping neck region reveal that the sloping neck does not provide any advantage *in vitro*. However, considering *in vivo* that the theory is aimed at the bone covering above the angled neck region, it would not be appropriate to evaluate this feature only biomechanically.

This study also evaluated tissue-level implants with a machined surface in the implant's cervical collar. The literature reports studies where implants with machined surfaces may be exposed to more torque, but the effects of the machined surface on biomechanics are not completely demonstrated (25). Chang et al. (26) investigated stress distribution of two different dental implant systems with tissue level and bone level cervical collars, and reported that the tissue-level implant system produced greater stresses than the bone-level implant system in type IV cortical bone, but they were almost equal in type II bone. However, the bone-level implant system produced greater stresses in cancellous bone, regardless of the type of loading angle or bone quality. Mosavar et al. (13) stated that stress distribution around the tissue-level implants is more evenly distributed and of a lower magnitude, thus, lower stress in the peri-implant bone may reduce the risk of marginal bone resorption around the implants. Sun et al. (25) found that the increase in machined surface height reduced the Pmax stresses in bones. It was noted that the lowest stresses in cortical bone occurred when the machined surface height ranged between 1.7 and 2.4 mm, and when it was less than 2.8 mm for the trabecular bone and on the implant. In the present study, the machined surface heights of the implants did not exceed 2.8 mm (R-Sw: 2.5 mm, R-St: 1.8 mm); however, in contrast to Sun et al. (25), tissue-level implants caused higher stresses on the bones. Moreover, with the increase in the neck section length, stress formation increased in direct proportion. Therefore, implants with a more extended neck section (Model R-Sw) reached the highest stress values in the study in terms of bony stresses. On the other hand, according to the Von Mises stress, tissue-level implants induced low stresses on itself.

Mosavar et al. (13) reported that maximum stresses were concentrated at the cervical cortical bone region and the first thread. In the present study, the stresses were observed to be distributed more intensely in the cortical bone. The cross-sections taken from the models depict that the stresses on the implants developed mostly in the neck region, though it also ensued in the internal connection, thread crests, and apex region (Fig. 4).

Ausiello et al. (4) reported that cortical bone is over-stressed when Pmax exceeds 30 MPa, and Pmin exceeds −60 MPa. In the same study, it was established that when Pmin or Pmax stress exceeded 5 MPa in trabecular bone, over-stress developed. In their study, Cicciù et al. (27) showed that different titanium overdenture retainer systems can withstand loads between 442 and 497 MPa without fracture. When evaluating stresses in the present study, it was observed that none of the stresses in either of the bones exceeded the specified limit values. For this reason, resorption was not expected to occur in any model under the present loading conditions. Although the Von Mises stress occurring against oblique forces in Model V-St (329 MPa) exceeded fatigue resistance of titanium, no overload was noted in other implants.

CONCLUSION

The results of the present study indicate the following.

1 Implants with reverse buttress thread and wider thread pitch (Group R) usually generate more stress on the cortical bone.
2 In trabecular bone, even if Pmax stress values arose a little higher for Group R, in general, the stresses remain at low levels for all the models.
3 V-threaded implants occurred more von Mises stress on itself.
4 Tissue level implants (model R-Sw and R-St) generated high stresses on bones and low stresses on itself. Besides, as the height of the neck section increases (model R-Sw), stress formation also increases.
5 Implants with a micro-threaded neck (V-As) caused low stresses on the cortical bone and high stresses on itself. Biomechanically, sloped neck design is not an advantage in terms of stresses in the cortical bone.

Different implant macrodesigns have their own advantages and disadvantages. However, considering the anterior region of the mandible often consists of dense cortical bone (D1 or D2), it may be advantageous to prefer implants with a V-thread design and a microthread neck surface, which creates less stress in the cortical bone.

REFERENCES

1. Alfadda SA, Al Amri MD, Al-Ohali A, Al-Hakami A, Al-Madhi N. Two-Implant-supported mandibular overdentures: do clinical denture quality and inter-implant distance affect patient satisfaction? Int J Prosthodont 2017;30:519-25.
2. Fernandez-Estevan L, Selva-Otaolaurruchi EJ, Montero J, Sola-Ruiz F. Oral health-related quality of life of implant-supported overdentures versus conventional complete prostheses: Retrospective study of a cohort of edentulous patients. Med Oral Patol Oral Cir Bucal. 2015;20:e450-8. doi:
3. Abuhussein H, Pagni G, Rebaudi A, Wang HL. The effect of thread pattern upon implant osseointegration. Clin Oral Implants Res 2010;21:129-36.
4. Ausiello P, Franciosa P, Martorelli M, Watts DC. Effects of thread features in osseo-integrated titanium implants using a statistics-based finite element method. Dent Mater 2012;28:919-27.
5. Chowdhary R, Halldin A, Jimbo R, Wennerberg A. Evaluation of stress pattern generated through various thread designs of dental implants loaded in a condition of immediately after placement and on osseointegration--an FEA study. Implant Dent 2013;22:91-6.
6. Ryu HS, Namgung C, Lee JH, Lim YJ. The influence of thread geometry on implant osseointegration under immediate loading: a literature review. J Adv Prosthodont 2014;6:547-54.
7. Ormianer Z, Matalon S, Block J, Kohen J. Dental Implant Thread Design

and the Consequences on Long-Term Marginal Bone Loss. Implant Dent 2016;25:471-7.
8. Lima de Andrade C, Carvalho MA, Bordin D, da Silva WJ, Del Bel Cury AA, Sotto-Maior BS. Biomechanical Behavior of the Dental Implant Macrodesign. Int J Oral Maxillofac Implants 2017;32:264-70.
9. Jimbo R, Tovar N, Anchieta RB, et al. The combined effects of undersized drilling and implant macrogeometry on bone healing around dental implants: an experimental study. Int J Oral Maxillofac Surg 2014;43:1269-75.
10. Degerliyurt K, Simsek B, Erkmen E, Eser A. Effects of different fixture geometries on the stress distribution in mandibular peri-implant structures: a 3-dimensional finite element analysis. Oral Surg Oral Med Oral Pathol Oral Radiol Endod 2010;110:e1-11.
11. Unsal GS, Erbasar GNH, Aykent F, Ozyilmaz OY, Ozdogan MS. Evaluation of stress distribution on mandibular implant-supported overdentures with different bone heights and attachment types: A 3D Finite Element Analysis. J Oral Implantol 2019;45:363-70. doi: 10.1563/aaid-joi-D-19-00076
12. Chowdhary R, Halldin A, Jimbo R, Wennerberg A. Influence of micro threads alteration on osseointegration and primary stability of implants: A FEA and in vivo analysis in rabbits. Clin Implant Dent Relat Res 2015;17:562-9.
13. Mosavar A, Ziaei A, Kadkhodaei M. The effect of implant thread design on stress distribution in anisotropic bone with different osseointegration conditions: a finite element analysis. Int J Oral Maxillofac Implants 2015;30:1317-26.
14. Ferreira MB, Barao VA, Delben JA, Faverani LP, Hipolito AC, Assuncao WG. Non-linear 3D finite element analysis of full-arch implant-supported fixed dentures. Mater Sci Eng C Mater Biol Appl 2014;38:306-14.
15. Kong L, Zhao Y, Hu K, et al. Selection of the implant thread pitch for optimal biomechanical properties: A three-dimensional finite element analysis. Advances Engineering Software 2008;40:474-78.
16. Ma P, Xiong W, Tan B, et al. Influence of thread pitch, helix angle, and compactness on micromotion of immediately loaded implants in three types of bone quality: a three-dimensional finite element analysis. Biomed Res Int 2014;2014:983103.
17. Lekholm U, Zarb GA. Patient selection and preparation. In: Branemark PI, Zarb GA,Albrektsson T, editors. Tissue integrated prostheses: osseointegration in clinical dentistry. Chicago: Quintessence Publishing Co; 1985. p. 199–209.
18. Misch CE. Density of Bone: Effect on treatment planning, surgical approach, and healing. Contemporary Implant Dentistry. St. Louis (US): Mosby; 1994.
19. Lan TH, Du JK, Pan CY, Lee HE, Chung WH. Biomechanical analysis of alveolar bone stress around implants with different thread designs and pitches in the mandibular molar area. Clin Oral Investig 2012;16:363-9.
20. Yalcin M, Kaya B, Lacin N, Ari E. Three-Dimensional Finite Element Analysis of the effect of endosteal implants with different macro designs on stress distribution in different bone qualities. Int J Oral Maxillofac Implants 2019;34:e43-e50.
21. Al-Thobity AM, Kutkut A, Almas K. Microthreaded Implants and Crestal Bone Loss: A Systematic Review. J Oral Implantol 2017;43:157-66.
22. Nickenig HJ, Wichmann M, Happe A, Zoller JE, Eitner S. A 5-year prospective radiographic evaluation of marginal bone levels adjacent to parallel-screw cylinder machined-neck implants and rough-surfaced microthreaded implants using digitized panoramic radiographs. J Craniomaxillofac Surg 2013;41:564-8.
23. Markose J, Suresh S, Eshwar S, Rekha K, Jain V, Manvi S. Comparison of platform switched and sloping shoulder implants on stress reduction in various bone densities: Finite Element Analysis. J Contemp Dental Practice 2017;18:510515.
24. Markose J, Eshwar S, Srinivas S, Jain V. Clinical outcomes of ultrashort sloping shoulder implant design: A survival analysis. Clin Implant Dent Relat Res 2018;20:646-52.
25. Sun Y, Kong L, Hu K, et al. Selection of the implant transgingival height for optimal biomechanical properties: a three-dimensional finite element analysis. Br J Oral Maxillofac Surg 2009;47:393-8.
26. Chang SH, Huang SR, Huang SF, Lin CL. Mechanical response comparison in an implant overdenture retained by ball attachments on conventional regular and mini dental implants: a finite element analysis. Comput Methods Biomech Biomed Engin 2016;19:911-21.
27. Cicciù M, Cervino G, Milone D, Risitano G. FEM Analysis of dental implant-abutment interface overdenture components and parametric evaluation of Equator and Locator prosthodontics attachments. Materials (Basel). 2019;12.